Ultrapure wood nanocellulose – assessments of coagulation and initial inflammation potential

Henriette R. Nordli[a], Brita Pukstad[a,b], Gary Chinga-Carrasco[c], Anne M. Rokstad[a,d,e*],*

[a]Department of Clinical and Molecular Medicine, Norwegian University of Science and Technology, Trondheim, Norway

[b]Department of Dermatology, St. Olavs Hospital, Trondheim University Hospital, Norway

[c]RISE PFI, Høgskoleringen 6b, NO-7491 Trondheim, Norway

[d]Centre of Molecular Inflammation Research, Trondheim, Norway

[e]Clinic of Surgery, Centre for Obesity, St. Olavs University Hospital, Trondheim, Norway

ABSTRACT

Using a lepirudin-based human whole blood model we evaluated the initial inflammatory and coagulation responses of dense and porous ultrapure (<50 endotoxin units/grams) cellulose nanofibrils (CNF), of carboxylated grade. The CNF was compared to the wound dressing AquaCel®, since it is a potential wound healing material. The porous CNF aerogels induced the strongest coagulation potential measured as prothrombin factor 1.2 (PTF1.2). AquaCel® induced the strongest complement response by terminal complement complex (TCC) and surface C3c. All materials activated leukocytes CD11b, while the levels of only three of 27 cytokines were significantly changed, limited to; i) an elevation of the monocyte chemoattractant protein-1 (MCP-1/CCL) by the CNF aerogel, ii) a reduction of eosinophil chemotactic proteins (eotaxin/CCL11) by the CNF aerogel and iii) a reduction of platelet-derived growth factor BB (PDGF-BB) by all CNF materials. In conclusion, the CNF materials and AquaCel® differently activate coagulation, complement and cytokines, improving the selection possibilities in various treatment situations of wound healing.

KEYWORDS

Coagulation, complement, cytokines, human whole blood model, ultrapure cellulose nanofibrils, wound dressings

1 INTRODUCTION

Nanocellulose has attracted much attention for its potential use as material for biomedical applications.[1,2] Bacterial nanocellulose (BNC) has shown promise as material to be used in wound healing,[3] but the production has been rather limited due to low yields and high cost.[1,4] As an alternative source, wood cellulose nanofibrils (CNF), has been suggested as a wound dressing material.[2,5,6] It can be produced in large quantities by well-established procedures.[5-Error! Reference source not found.7] Chemical pre-treatment yields CNF widths less than 20 nm and lengths in the micrometer scale.[8] The nanomaterial forms strong, translucent structures and is able to maintain a moist environment. TEMPO-mediated oxidation is a relatively common pre-treatment used to facilitate the production of CNF,[7] and the material have been used in a series of studies focusing on biomedical applications.[5,9-16] Various types of CNF are compatible with different cell types in the terms of low cytotoxicity.[5,17-21] Previously we have produced ultrapure wood CNF containing low levels of endotoxins (45 endotoxin units/g CNF), and demonstrated that this material was compatible with human keratinocytes and fibroblasts of relevance in wound healing applications.[22] Different cells and blood components are active in the early phase of wound healing.[23] The interactions between these elements and the potential wound dressings needs clarification in order to design optimized materials for effective wound repair. In particular, the material influence on the leukocytes responses and the blood proteins needs exploration.

Blood proteins or body fluids will immediately adsorb to a biomaterial surface upon contact. Depending on the materials, physiochemical properties, the proteins can be conformation changed and activated.[24,25] Zymogens of blood coagulation and complement systems are easily activated proteins. Of the most reactive zymogens are coagulation factor XII (FXII) and complement 3 (C3), thus both these cascades might be activated to various extents. The

complement cascade also communicates closely with leukocytes, where the activated products anaphylatoxins (C3a, C5a) are attractors and modulators of the immune responses.[25] C5a is a particularly strong chemoattractor of granulocytes and monocytes, and both C3 and C5 have been shown to augment wound healing.[26] Although complement activation is needed to restore tissue injury, inappropriate complement activation can contribute to further tissue damage, for instance in chronic wounds.[27]

Previous studies of the hemocompatibility of bacterial cellulose and mixed products containing bacterial cellulose in blood-contact devices points to some coagulation and complement activation potential.[28-31] Recently, exploration of coagulation and complement reactivity by TEMPO oxidized nanocellulose was explored in the blood chamber model.[32] However, information on proven ultrapure TEMPO CNF involving the inflammatory potential of leukocytes are still lacking. The purity is of relevance when used in biomedical devices, and is of highly importance when evaluating the leukocyte reactivity. A physiologically relevant model exploring the initial inflammatory responses is the lepirudin based human whole blood model.[33] This model used to characterize the inflammatory properties of biomaterials is valid for measuring the leukocytes and complement reactivity[34,35]. The model has also proved valuable in exploring both the FXII driven intrinsic and monocyte-tissue factor driven extrinsic pathway of coagulation.[36] In the present study, we used this model exploring ultrapure TEMPO CNF materials by focusing on the potential to activate coagulation, complement and leukocytes. These are central factors of wounds and wound healing repair. We emphasize that increased knowledge about the behavior of human blood in contact with proven ultrapure CNF is required for proper selection of materials, to improve the treatments of non-healing wounds.

2 EXPERIMENTAL

2.1 Materials

Never dried *Pinus radiata* kraft pulp was kindly provided by CMPC (Chile), while NaBr was from Merck and sodium hypochlorite was from Fisher Scientific. 2,2,6,6-tetramethylpiperidinyl-1-oxyl (TEMPO), phosphate-buffered saline (PBS), PBS with calcium and magnesium, ethylenediaminetetraacetic acid (EDTA) and paraformaldehyde were all purchased from SigmaAldrich (St. Louis, MO, USA). Non-pyrogenic sterile saline (0.9% NaCl) and endotoxin free, non-pyrogenic, water from B. Braun (Melsungen, Germany). The anti-coagulant lepirudin (Refludan) was obtained from Celgene Europe (Windsor, GB). Antibodies had the following specification: anti-CD14 FITC, PE anti-CD11b phycoerythrin, PE mouse IgG control all from BD BioSciences (San Jose, CA, USA). Aantihuman C5b-9 clone aE11 (Diatec, Oslo, Norway), and biotinylated 9C4 was an in-house made antibody as described in.[37] FITC-conjugated polyclonal rabbit anti-human C3c (F0201) was provided by Dako (Glostrup, Denmark) and the control antibody was a FITC-conjugated rabbit polyclonal anti-mouse IgG (F0261), both from Dako (Glostrup, Denmark). Sheep α-human Factor H was purchased from Binding Site (San Diego, CA, USA) and the secondary antibody CF633-conjugated α-sheep IgG was provided by Sigma Aldrich. Streptavidin was from BioLegend (San Diego, USA) and substrate reagent A and B from R&D Systems (Minneapolis, USA). Commercial ELISAs used were Enzygnost F1 + 2 (monoclonal, OPBD035) Siemens Healthcare AS (Marburg, Germany), and Bio-Plex Human Cytokine 27-Plex Panel from Bio-Rad (Oslo, Norway). Equipment for blood: Polypropylene vials (NUNC, Roskilde, Denmark) with BD vacutainer tops and BD vacutainer glass (Belliver Industrial Estate, Plymouth, UK) used for blood sampling and glass control, respectively.

2.2 Nanocellulose production

The production of an ultrapure CNF material has been reported in our previous study.[22] Shortly described, the raw material was a never dried, fully bleached, 100% Pinus radiata pulp fibers, with a carbohydrate composition being composed by 87% cellulose, 12.2% hemicellulose and 0.8 % lignin.[38] The fibers were washed with MQ water (25 l) on a Büchner funnel with filter cloth. Fibers (2.5%) were autoclaved in 0.1 M NaOH for two hours and then washed with MQ water (25 l) three times. 2,2,6,6-tetramethylpiperidinyl-1-oxyl (TEMPO) mediated oxidation, using 3.8 mmol hypochlorite (NaClO) per gram cellulose was performed.[7] Autoclaving in NaOH combined with TEMPO mediated oxidation treatment is an effective way of removing endotoxins. Hence, the TEMPO CNF tested in this study contains 45 endotoxin units/gram (EU/g) cellulose and is defined as ultrapure as previously reported.[22] We have previously reported the degree of polymerization (DP), and the carboxyl and aldehyde content to be 709, 855 µmol/g cellulose and 71 µmol/g cellulose, respectively, when applying the same pulp fibers and TEMPO mediated oxidation procedure.[10] Homogenization was performed using an ultra-turrax, with 24 000 rpm for 6 min, on a dispersion of 2%. For clarity purposes we will refer to the ultrapure nanocellulose material produced in this study as CNF.

2.3 CNF characterization

The CNF dispersion was diluted to 0.01% and prepared for AFM and STEM analyses. A drop of the sample was deposited on a clean glass slide and dried overnight. The glass slide with the CNF was imaged with AFM. AFM imaging was performed with a Multimode AFM (with Nanoscope V controller), Digital Instrument. All images were recorded in ScanAsyst mode (peak force tapping mode), at room temperature in air. The AFM tips of spring constant value ~0.4 N/m were purchased from Bruker AFM probes. The image size was 2x2 µm, with a

resolution of 1.95 nm/pixel. The AFM was performed on individualized CNFs attached to the glass slide in order to measure the height at 100 local positions.

Additionally, cobber grids were immersed in the 0.01% suspension of the CNF sample, stained with uranyl acetate and imaged with a S(T)EM was a Hitachi S-5500 electron microscope. The acceleration voltage was 30 kV. The images were acquired in bright field mode. Totally, 104 randomized measurements of single CNFs were undertaken from 13 S(T)EM images.

Cross-sections of films and aerogels were prepared with a Hitachi ion-milling equipment (IM4000). The milling time was 5 hours at 2.5 kV. The samples were covered with a thin layer of gold and cross-sectional images were acquired at various magnifications with a Hitachi scanning electron microscope (SEM, SU3500), in secondary electron imaging mode.

In this study, conductometric titration was used for measuring the carboxylic acid group content of the ultrapure CNF and AquaCel® (a commercial wound dressing).[39]

2.4 Preparation of cellulose samples and controls for evaluations

The CNF dispersions (0.2 wt%) were either dried at room temperature to form dense films, or frozen down (-20 or -80 ºC) and thereafter freeze-dried to form aerogels with varying porosities. The grammage of the film and aerogels was 20 g/m². For simplicity purposes, aerogels freeze-dried at either -20 or -80 ˚C are referred to as AG-20 and AG-80, respectively. From these samples, punch biopsies (6 or 8 mm) where used to make small circular samples. AquaCel® was also used for comparison, and circular samples (8 mm) were punched out. AquaCel® consists of hydrofibers, which is a soft, non-woven dressing composed of sodium

carboxymethylcellulose.[40] All these circular samples were washed in ethanol (70%) and then with PBS five times. The CNF samples of 8 mm and 6 mm diameter weighed 1 mg and 0.57 mg respectively, whereas the AquaCel® sample of 8 mm weighed 4.8 mg. Each material sample was finally embedded in 100 µl sterile and pyrogen-free PBS using 1.8 ml sterile polypropylene vials (Nunc), and finally 100 µl sterile and pyrogen-free PBS (with $CaCl_2/MgCl_2$) was added giving a final volume of 200 µl in each samples. The negative control sample contained PBS (200 µl) only, and reflects the background activation by the polypropylene vials used for blood incubation. The positive controls were heat inactivated gram negative bacteria *E. coli* and glass. *E. coli* is a broad activator that triggers inflammatory cytokines, complement as well as coagulation.[41-43] Glass is a well-known activator of the contact pathway of coagulation mediated through factor XII.[36] *E. coli* was beforehand washed and stored in PBS, and upon use diluted to give 0.7×10^7 bacteria's pr sample (final concentration adding blood of 1×10^7/ml.) As glass control, sterile glass tubes added PBS (100 µl) in addition to PBS (with $CaCl_2/MgCl_2$, 100 µl) was used.

2.5 Whole blood model

The lepirudin whole blood model is based on inhibition of thrombin to avoid coagulation, while the complement cascade is fully active and interacting with the leukocytes, particularly through the activated complement anaphylatoxins (C3a and C5a) binding to the leukocytes receptors C3aR, C5aR1 and C5aR2,[44,45] and also are involved in the regulation of cytokine responses through cross-talking with pattern recognition receptors of the toll-like receptors.[46] The coagulation cascade upstream thrombin is also rendered intact and able to be activated as well as possessing cross-talking with the complement system.[36,43] The experiments were conducted as described by Mollnes et al.,[33] using lepirudin (50 µg/ml) as anticoagulant. Fresh blood from six healthy volunteers withdrawn into low activating polypropylene Nunc tubes

(4.5 ml) were used. For each sample, 500 µl blood was added and incubated between 0, 60, 120, 240 and 360 min under continuous rotation at (37 ºC). After incubation, further complement and coagulation activation was inhibited by adding EDTA (10 mM final concentration). Finally, blood was centrifuged at 1500G 15 min, and plasma harvested and stored at -20 ºC before analysis. The baseline value represents the values measured from the blood immediately after retraction following the inactivation by EDTA. This value is representing the value closest to the factors as they appear in circulation. The PBS has been incubated for given time lengths, and represents the background control of the polypropylene material incubated at the same time lengths as the CNF samples and AquaCel®. PBS is thus the most appropriate control in this specific testing.

2.5.1 Coagulation activation

Prothrombin fragment 1.2 (PTF1.2) is a small peptide fragment formed upon prothrombin cleavage to thrombin during activation, and is therefore a measure on the materials total ability to activate coagulation through contact or tissue factor pathway. Enzygnost* F 1+2 (monoclonal) assay was used to measure PTF1.2. The assay was performed according to the protocol, with dilution of the plasma in the range of 10-1000 x depending on the activity.

2.5.2 TCC

The terminal fluid phase C5b-9 complex (TCC) was quantified by an immunoassay described in detail previously,[47] with later modifications.[48]

2.5.3 Surface C3 deposition and factor H binding

Samples of CNF (8 mm) stored in 200 µl sterile NaCl (0.9 %), were incubated in pooled (N= 5) lepirudin anti-coagulated plasma (600 µl) for 4 h at 37 ˚C under constant rotation. Staining

of C3c deposition was by adding 100 µl FITC-conjugated rabbit anti-human C3c (50 µg/ml) or FITC-conjugated rabbit anti-mouse IgG (control) for 30 min. Factor H binding was evaluated using Sheep anti-human Factor H (50 µg/ml) followed by secondary CF633-conjugated IgG (10 Ig/ml) for 30 min. The secondary CF633-conjugated IgG was used as control. For each step the samples were washed twice with 0.9% NaCl. Visualization of deposition of C3c or associated factor H was by a Zeiss LSM 510 confocal microscope equipped with a 488 nm Argon and a 543 nm HeNe laser (Carl Zeiss MicroImaging GmbH, Göttingen, Germany).

2.5.4 Leukocyte CD11b expression

After 60 min incubation in whole blood of the various materials, blood (50 µl) was retracted and fixed with 1 % PFA in an equal volume for 4 min (37 ºC) and further staining (15 min) with PE anti-CD11b+ FITC anti-CD14, or as control PE mouse IgG 2α + FITC anti-CD14. This was followed by lysis of red blood cells in 1 ml lysisbuffer for 15 min. Analyses were performed on a flow cytometer (Beckman Coulter Epics XL-MCL, Coulter Corp, FL) by gating the granulocytes and monocytes in a SSC/FITC anti-CD14 dot plot, and giving CD11b expression as mean fluorescence intensity (MFI).

2.5.5 Multiplex immunoassay

Lepirudin plasma harvested after 360 min incubation were analyzed with Bio-Plex Human Cytokine 27-Plex Panel for quantification of tumor necrosis factor (TNF), interferon gamma (IFN-γ), interleukin-1 beta (IL-1β), IL-1 receptor antagonist (IL-1RA), IL-2, IL-4, IL-5, IL-6, IL-7, IL-8 (CXCL8), IL-9, IL-10, IL-12p70, IL-13, IL-15, IL-17, monocyte chemoattractant protein 1 (MCP-1/CCL2), chemokine ligand 10 (IP-10/CXCL10), regulated upon activation T-cell expressed and secreted (RANTES/CCL5), macrophage inflammatory protein-1-alpha

(MIP-1α/CCL3), macrophage inflammatory protein-1-beta (MIP-1β/CCL4), granulocyte colony stimulating factor (G-CSF), granulocyte-macrophage colony stimulating factor (GM-CSF), eosinophil chemotactic proteins (Eotaxin/CCL11), basic fibroblast growth factor (bFGF), vascular endothelial growth factor (VEGF) and platelet derived growth factor-BB (PDGF-BB) according to the manufacturer's protocol using the half volume of reagents.

2.6 Statistics

Results were analyzed using GraphPad Prism Software, version 5. Each sample in the whole blood model test was compared with the PBS control at the corresponding time-point (N=6). A two-way ANOVA followed by Bonferroni post-test was chosen to take into account the three time points in addition to the various samples. Each cytokine measured in the different samples were compared with the PBS control (N = 6) and a one-way ANOVA followed by Dunnet's multiple comparison test was chosen for this. We assumed that the data were not normally distributed due to the low number of replicates (N=6), therefore the data were log-transformed before analysis. In addition, each sample and control were compared to each other using either a 1-way or a 2-way ANOVA followed by the Bonferroni post-test. Values at $p < 0.05$ or less were considered statistically significant.

2.7 Ethics

The use of human whole blood for basal experiments was approved by the Regional Ethics Committee for medical and health research ethics under REK2009/2245 in accordance with their recommendations.

3 RESULTS

3.1 Characterization of CNF and AquaCel®

The carboxylic acid group content of CNF and Aquacel® was 882 and 1350 µmol/g, respectively.

The three different types of CNF wound dressing samples as well as AquaCel® were characterised by visual inspection (punch biopsies) and SEM as shown in Fig. 1. SEM inspection revealed that the AG-20 sample (Fig. 1F and J) had lower porosity (fewer and bigger pores) than the AG-80 sample (Fig. 1G and K), which had a bulkier structure caused by a greater amount of smaller pores. This was also confirmed by the thickness of the AG-20 (~1 mm, Fig. B and F) compared to AG-80 (thickness ~2 mm, Fig. 1C and G), considering that all the CNF dressing samples were manufactured with the same mass (20 g/m^2). The air-dried film was considerably thinner (thickness ~20 µm) and had a dense structure (Fig. 1A, E and I). The commercial wound dressing AquaCel® consists of hydrofibers (Fig. 1D, H and L), composed of sodium carboxymethyl cellulose, which is incorporated in the form of a fleece held together by a needle-bonding process.[40]
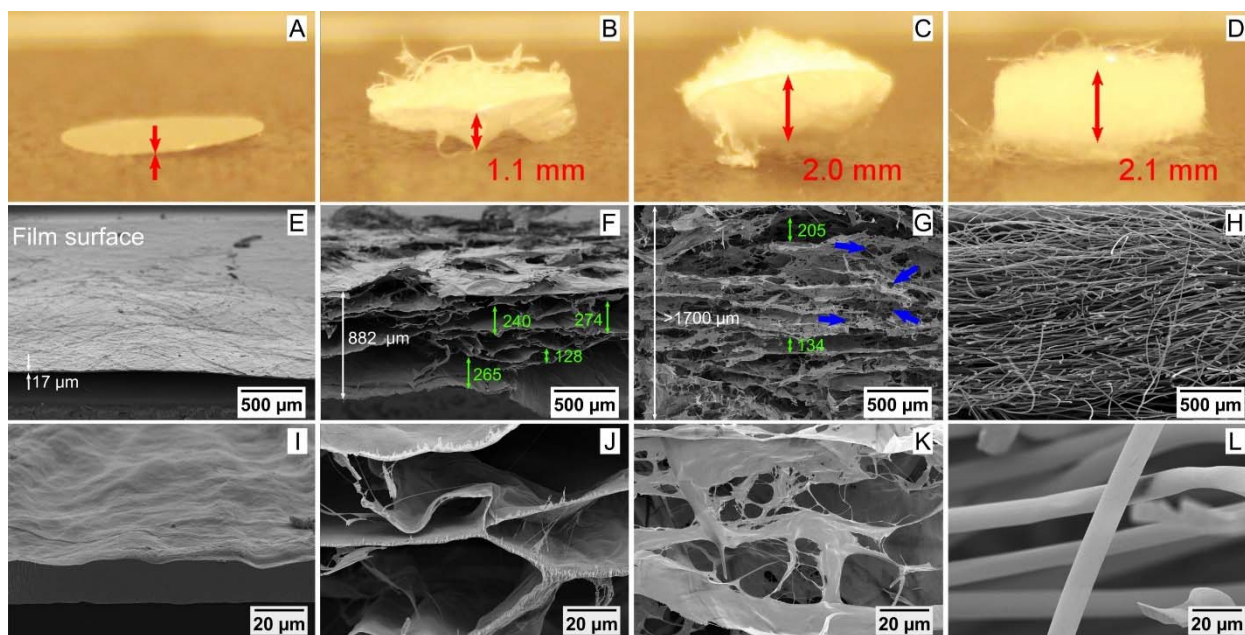
Figure 1. Structure characterization of the ultrapure CNF material and AquaCel®. Photos of punch biopsies (6 mm) exemplifying the local thickness (red arrows) of the four assessed samples; CNF film (A), AG-20 (B), AG-80 (C) and AquaCel® (D). Porosity assessed by SEM for the CNF film (E and I), AG-20 (F and J), AG-80 (G and K) and AquaCel® (H and L). The middle panel shows images acquired at 50× magnification. The lower panel shows images acquired at 1000× magnification. The white arrows in E, F and G show the local thickness of the CNF structures. The yellow arrows exemplify some local pore heights in B and C, given in micrometers. The white/red arrows in (G) exemplify some small pores that appear due to the low freezing temperature (-80 °C).
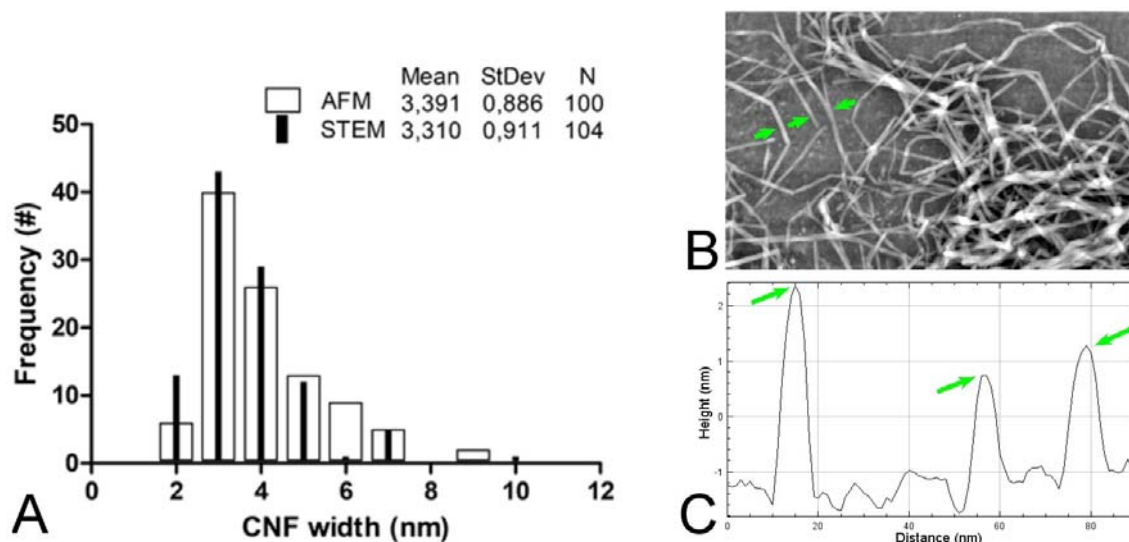
Figure 2. Nano-characteristics of the CNF material quantified with AFM and STEM (A). An AFM image exemplifying the nano-morphology of single nanofibrils (B). The heights of single nanofibrils (C) measured at the locations marked with green arrows in (B).

The AFM analysis performed in this study confirms the nano-characteristics of the ultrapure CNF (Fig 2.). The quantification is also confirmed by STEM data, thus giving supportive evidence of the nanofibril widths, i.e. 3.4 nm (±0.9 nm) and 3.3 nm (±0.9 nm) based on AFM and STEM data, respectively (Fig. 2A). This assessment indicates the morphology of elementary fibrils that have been reported to be 3.5 nm, confirmed for *P. radiata* pulp fibres.[49]

3.2 Coagulation activation

The coagulation activation potential upstream thrombin is reflected in the materials ability to induce PTF1.2. The CNF materials AG-80 and AG-20 were the most rapid and potent inducers of PTF1.2 (Fig. 3A, 3B and Supporting Information Table S1-S2). The CNF film induced a far slower induction of PTF1.2 (Fig 3A and 3B). After 240 min incubation, all materials showed significantly (p<0.001) elevated values compared to the PBS-control (Fig 3B). The 6 mm materials induced slightly lower amounts of PTF1.2 than the corresponding 8

14

mm materials, but not significantly different, and with overall the same patterns of activation. AquaCel® induced a slower activation of PTF1.2 than the CNF materials, with an activation pattern similar as *E. coli* (Fig. 3B). Comparing the different activation levels between the materials at given time points, the AG-20 and AG-80 were significantly more potent than the film at 60-120 min (60 min $p<0.01$ or $p<0.001$, 120 min $p<0.05$ or $p<0.01$), while not after 240 min (Supporting Information Table S2). The AG-20 and AG-80 (8mm) were also significantly elevated to AquaCel® at the earliest time points (60 min $p<0.05$ or $p<0.001$, 120 min $p<0.001$), but not after 240 min. The film, AquaCel® and *E. coli* demonstrated a similar response pattern, and no significant differences were achieved between these materials at any time point (Table S2). Of note, *E. coli* mainly trigger coagulation through the monocyte TF-pathway.[36,50] The porous CNF materials showed a rapid response pattern of activation similar to the positive control glass. Of note, glass is a known activator of the FXII pathway of coagulation.[36] While glass showed a significant elevated activation in comparison to AG-20 at the earliest time-points (60 min $p<0.05$), no significance was achieved in comparison to AG-80, pointing to an induction potential comparable to glass.
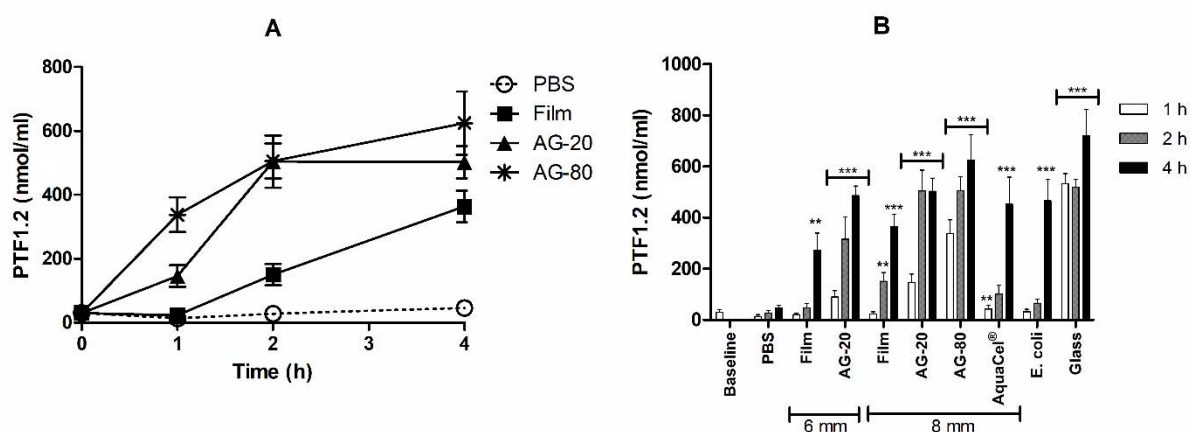

Figure 3. Effect of CNF on coagulation activation (PTF1.2) after incubation in human whole blood. (A) Time dependent effects of the CNF materials (8mm) in comparison to PBS. (B)

Overview of all tested CNF materials (6 and 8 mm), the wound dressing AquaCel®, and the positive controls *E. coli* and Glass. Results are given as means ± SEM (N = 6). Significant different (**p<0.01, ***p<0.001) as compared to the PBS control. All the values are given in Supporting Information Table S1, while statistical significant comparisons between all the samples and controls are given in Table S2.

### 3.3 Complement activation

The complement activating potential measured by the fluid phase TCC is given in Fig. 4. The time kinetics showed that the AG-80 and AG-20 were more potent inducers of TCC than the CNF film (Fig. 4A). A comparison of the various material and controls presented in Fig. 4B. The AG-20 and AG-80 materials induced statistical significant (p<0.001) increase of TCC as compared to the PBS control at all time points, and at similar levels as for the positive control *E.* coli (no statistically differences). The induction of TCC by the film (6 or 8 mm) were at the same level as the PBS control with no statistically significant difference. In comparison to *E. coli*, the film (both 6mm and 8mm) were statistically lower (p<0.001) at all time points (Supporting Information Table S3 and S4). The most potent TCC inducer was AquaCel®, which was significantly (p<0.001 at all time points) more elevated than *E. coli* (Fig. 4B). AquaCel® was also significantly elevated (p<0.001 at all time points) in comparison to all the CNF materials. The AG-20 and AG-80 materials were both significant elevated (p<0.001) as compared to the film (both 6mm and 8mm) at all time points. These data altogether points to differences in the responding patterns to complement.
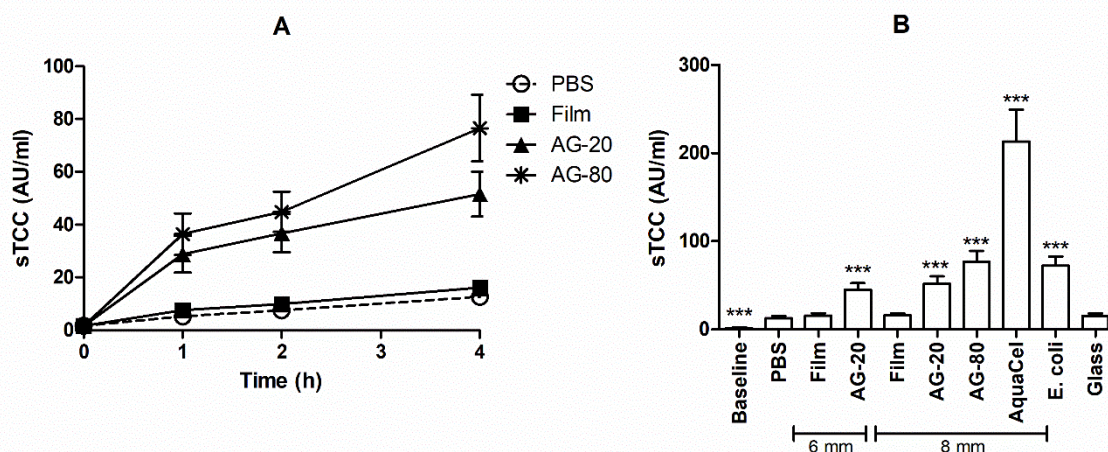
Figure 4. Effect of CNF materials on the amounts of fluid phase terminal complement complex (TCC) after incubation in human whole blood. (A) TCC as a function of time with CNF materials (8 mm) in comparison to PBS. (B) Comparison of the TCC amounts between the CNF materials (6 and 8 mm) with the wound dressing AquaCel®, *E. coli* and Glass after 240 min incubation. Results are given as means ± SEM (N = 6). Significant different (*** p<0.001) as compared to the PBS control. All the values (including timepoint 1 and 2 h) can be found in Supporting Information Table S3, while statistical significant comparisons between all the samples and controls can be found in Table S4.

The surface reactivity of complement was evaluated by anti-C3c and factor H. On complement reactive biomaterials, C3c can be seen in spotted patterns from building the C3 convertase at the surface.[34] Factor H, is a complement-inhibitor binding to the activated C3b initiating the inactivation to iC3b,[51] but could also potentially bind directly to the material as previously demonstrated for sulfated alginates promoting anti-complement activity.[52] The deposition of complement C3c was evenly distributed on the CNF film (Fig. 5A) and on AG-20 (Fig. 5B), with a more prominent staining by the latter. The porous surface of AG-80 showed more spotted deposition pattern with higher intensity (Fig. 5C). AquaCel® showed an evenly

17

distribution of C3c, but with a stronger intensity as compared with the CNF materials (Fig. 5D). Factor H was not detected on any of the materials (Supporting Information Fig. S1). The data indicate a low ability of the CNF film to be associated with C3 or building the C3 convertase at the surface, while some more potential by the porous CNF materials (AG-20 and AG-80) at least to associate with C3. Data further indicate that the CNF surface does not have anti-complement activities by association to factor H.
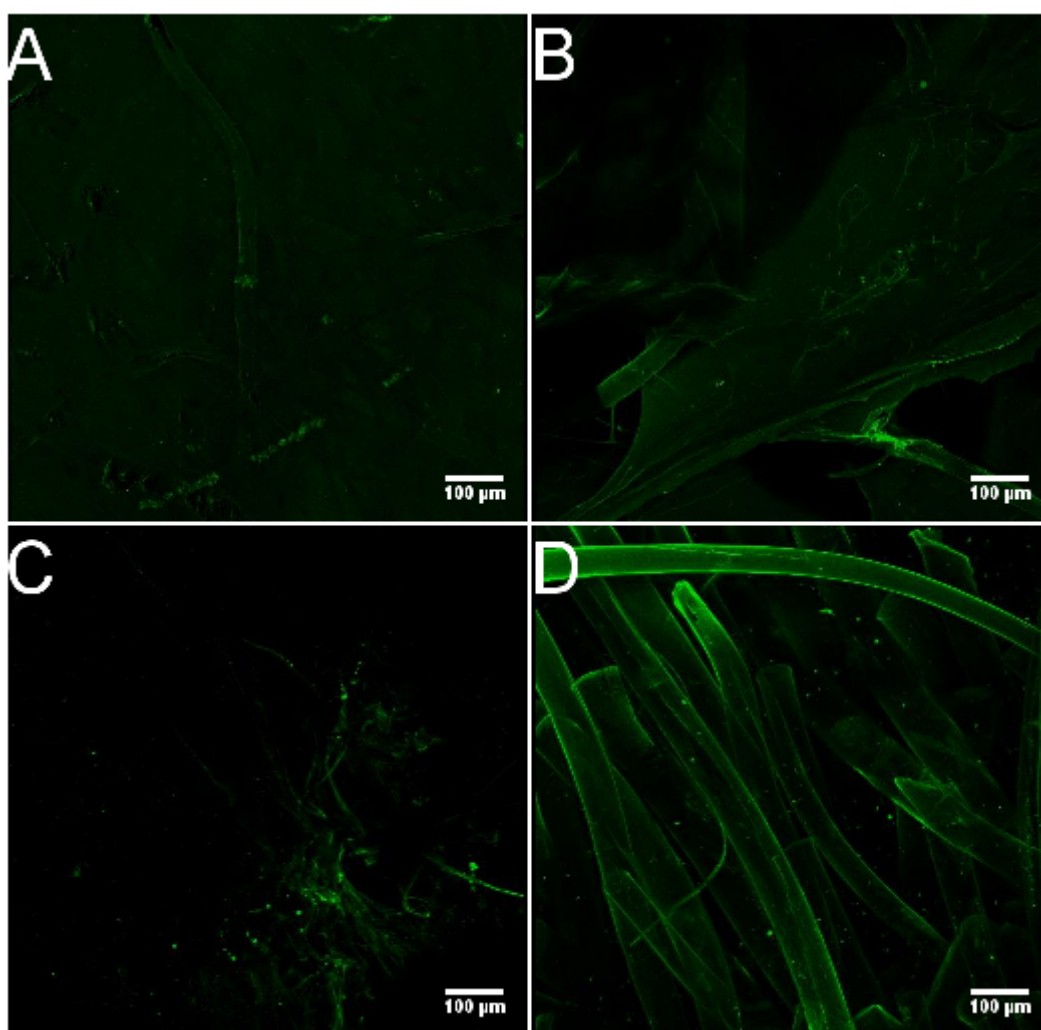
Figure 5. Confocal images of the CNF materials surface, Film (A), AG-20 (B), AG-80 (C), AquaCel® (D), with complement C3 deposition after 4 h incubation in lepirudin anticoagulated plasma. Images are given as 3D projections of scanned sections.

3.4 Leukocyte activation measured by CD11b and secreted cytokines

The complement receptor 3 (CR3) or CD11b/CD18 is an integrin receptor on monocytes and granulocytes elevated expressed upon activation. CD11b/CD18 is involved in cell attachment and phagocytosis mediated through activated complement (C3b/iC3b) or the peptide sequence RGD within fibrin and fibrinogen.[34] The ability of the CNF materials to potentiate CD11b expression is shown in Fig. 6. Of note, the elevation of CD11b in the PBS control as compared with the baseline value is reflecting the background activation by the polypropylene surface. All materials induced an elevation of CD11b in monocytes and the granulocytes as compared to the PBS control. In the monocytes, statistically significant ($p<0.05$) differences were obtained for the AG-20 (6mm) and the AG-80 (8mm) (Fig 6A). In the granulocytes, all the materials induced a statistically significant ($p<0.05$-0.001) elevation (Fig. 6B). Of note, no statistically differences between the materials, or to *E. coli* could be found (Supporting Information Tables S5 and S6).
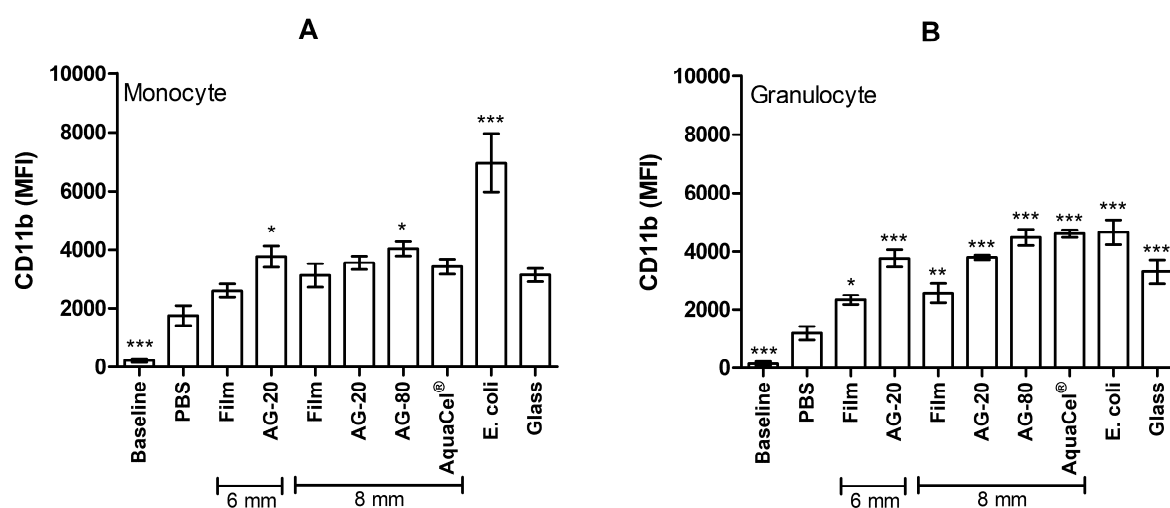

Figure 6. CD11b expression in human monocytes and granulocytes following 1 h exposure of CNF materials and controls measured by flow cytometry. (A) Monocyte and (B) granulocyte. Means ± SEM (N = 6). Significant different (* $p<0.05$, ** $p<0.01$, *** $p<0.001$) as compared to the PBS control. All the values can be found in Supporting Information Table S5, while

statistical significant comparisons between all the samples and controls can be found in Table S6.

Among the 27 cytokines evaluated, the investigated CNF materials only induced significantly elevation in one cytokine, the chemokine MCP-1/CCL2 upon blood contact with the CNF aerogels AG-20 and AG-80 of 8 mm sizes (Fig. 7A and Supporting Information Fig S2). In contrast, the positive control, *E. coli* induced a significant elevation of 15 cytokines (Supporting Information Fig. S2), but among these were not MCP-1/CCL2. On the other side, the plasma concentrations of PDGF-BB and Eotaxin/CCL11 was lowered upon exposure by the CNF materials, whereas not after the exposure to AquaCel® or *E. coli* (Fig. 7B-C). More specifically, all CNF materials significantly reduced the plasma amounts of PDGF-BB (Fig. 7B), while Eotaxin/CCL11 was significantly lowered by the AG-20 and AG-80 (Fig. 7C). No significant changes were found in the inflammatory cytokines IL-1β, TNF and IL-6, or the anti-inflammatory mediators IL-1RA and IL-10 by any of the materials, while these factors were elevated by *E. coli* (Supporting Information Fig S2). These cytokines are commonly induced by LPS (lipopolysaccharides, endotoxin) upon binding to the monocytes receptors CD14/TLR4,[53,54] thus the lack of stimulation of these cytokines is supported by the low endotoxin levels present in our materials. The growth factors VEGF or bFGF were not significantly changed by any of the materials, while significantly elevated by *E. coli* (Supporting Information Fig S2), again pointing to a low activating potential by the CNF material. For the T-cell secreted cytokines IL-2 and IL-4 a significant reduction was found for some samples of CNF materials (6 mm) (Supporting Information Fig S2). Comparing the CNF materials, the film (8 mm) showed significant (p<0.01, p<0.001) lower amounts of MCP-1/CCL2 and higher PDGF-BB (p<0.01) than the AG-20 and AG-80 (8 mm). AG-20 and AG-80 showed also significant lower PDGF-BB (p<0.001) and Eotoxin (p<0.01, p<0.001) as

compared to *E. coli*, and significant higher MCP-1/CCL2 (p<0.001) as compared to AquaCel®.

AG-80 also gave a significant higher MCP-1/CCL2 (p<0.05) as compared to *E. coli*. No

differences were found between the film and AquaCel®, whereas compared to *E. coli* only the

8mm showed a significant lowering (p<0.05) effect to PDGF-BB. In conclusion, the CNF

materials affected few of the 27 measured cytokines. Further on, AquaCel® induce no

significant changes in any of the mediators. The entire panel of cytokines is shown in

Supporting Information Fig. S2.
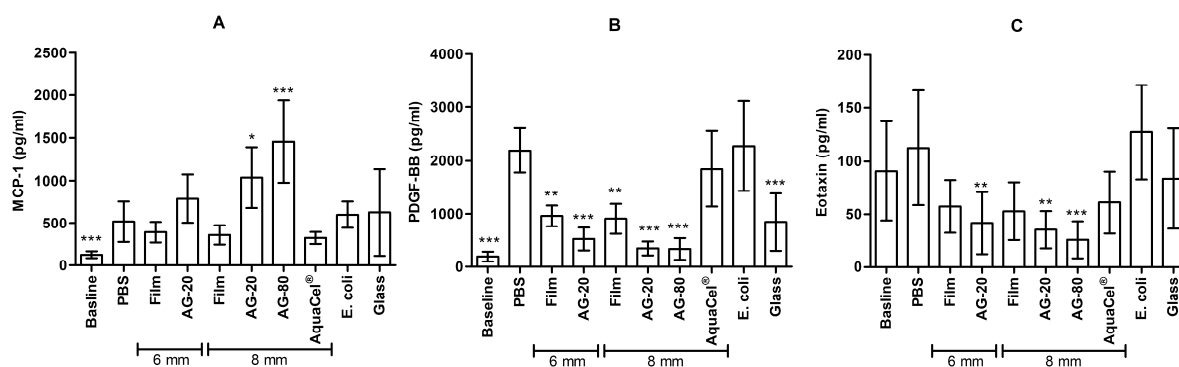
Figure 7. Cytokine induction (MCP-1/CCL2 (A), PDGF-BB (B), Eotaxin/CCL11 (C)) by the

CNF materials (film, AG-20 and AG-80, 6 and 8 mm) and controls in human whole blood after

360 min incubation. Results are given as means ± SEM (N = 6). Significant different (* p<0.05,

** p<0.01, *** p<0.001) as compared to the PBS control. All the values can be found in

Supporting Information Table S7, while statistical significant comparisons between all the

samples and controls can be found in Table S8.

4 DISCUSSION

Nanocellulose from wood represent a potential future material in non-healing wounds repair. Hence, it is of importance to clarify the effects of specific material designs on the initial blood reactions, of relevance for the wound healing process.

The structural assessment performed in this study based on AFM and STEM characterizations confirms the cellulose nanofibrils with diameters less than 10 nm, in agreement with.[7,8] The nanoscale dimensions of the nanofibrils are appropriate for the formation of porous materials. The air-dried film had a dense structure, while the aerogels were porous. AG-20 had lower porosity than AG-80. The porosity also is affected by the temperature applied to freeze the materials before the drying step. Martoïa et al.[55] demonstrated that rapid cooling (temperature < -40 °C) caused a nanofibrillar structure with higher homogeneity and smaller pores (between 1 and 60 nm), compared to freezing at higher temperature (-13 °C). Consequently, the results of Martoïa et al.[55] confirm the visual inspection performed in this study with SEM.

The effect of the varying porosities (from dense CNF films to porous CNF aerogels) and charge could be factors important for tailoring wound dressings with appropriate characteristics, by affecting the coagulation and complement reactivity. The CNF materials more potently activated coagulation and less potently complement in comparison to the commercial dressing AquaCel®. This is in consistence with the recent finding of Basu et al.[32] Moreover, these authors suggested that a rapid activation of coagulation is a beneficial trait in facilitating the wound-healing.[32] In supplement to Basu,[32] we extended the time-lengths of complement measurements and revealed complement reactivity by the porous CNF materials (AG-20 and AG-80). Although complement is involved in the wound repair, an inhibition of

complement might also facilitate the chronic wound healing.[27] The different profiles thus open for the possibility of material selection for better tailoring of the wound healing response. Particularly interesting was the significant variations in complement reactivity found between the CNF materials (film versus porous structures), and further to AquaCel®. This clearly points to a possibility for material selection and to tailoring of properties in along various needs during the non-healing wound treatment.

It is important to emphasize that our carboxylated CNF is considered ultrapure and contains 45 EU/g cellulose. This low content of endotoxins was only achieved with an additional washing and autoclaving in NaOH, before the TEMPO mediated oxidation procedure.[22] TEMPO mediated oxidation alone has not been capable of reducing the original endotoxin content to levels acceptable for biomedical use (Supporting Information Table S9). Our ultrapure CNF materials showed the ability to induce only one out of 27 cytokines, in contrast to the positive control *E. coli* were capable of inducing 15 cytokines. Before discussing these findings, it can be emphasized that when screening for cytokine profiles in a whole blood model, various response patterns are expected due to different stimulatory pathways (i.e. complement dependence, pattern recognition receptors dependence), cell-types, as well as induction of cytokines synthesis or release from granules storage. The cytokine levels in a whole blood system therefore reflect a multitude of effects including the specific stimulatory pathways as well as the physicochemical impact by the material.[33,35,36,43,56,57] The gram-negative bacteria *E. coli* exposes LPS in addition to representing a surface without complement regulators, and thus has the ability to both active the pattern recognition receptors (as CD14/TLR4) and complement with the possibilities of cross-talks.[54,56] Importantly, the lack of TNF, IL-1β and IL-6 induction in the whole blood system demonstrates the ultrapure nature of the CNF material tested in this study, since endotoxins would induce inflammatory cytokines.[58]

In contrast to *E. coli*, our porous quality CNF materials induced a significant secreted amount of MCP-1/CCL2, thus pointing a distinct stimulatory mechanism. Interestingly, MCP-1/CCL2 has been one among a broader range of inflammatory mediators (IL-1β, TNF, IL-6, IL-8, VEGF, MIP-1α) that has been activated following exposure of alginate/poly-L-lysine complexed materials in a complement dependent way.[35,57] MCP-1/CCL2 is an important monocyte chemoattractor, which might be of importance since monocytes play an active role in the wound healing inflammatory and resolution phase. The significant lowering of PDGF-BB and Eotaxin/CCL11 by the CNF materials might also be influencing the wound healing process through their potential impacts on fibroblast growth and eosinophilic chemotaxis, respectively.[23,59] PDGF-BB is a growth-factor produced by platelets and stored in their alpha granules ready to be released upon activation,[60] whereas Eotaxin/CCL11 is stored in Eosinophilic granules.[61] The significant lowering of PDGF-BB and partly by Eotaxin/CCL11 following exposure of the CNF materials could thus possibly be explained either by inhibition of granule release, or alternatively an absorption to the material surface. The complexity of cytokines and growth hormones during wound healing is not fully understood. PDGF-BB has been shown to have a possible positive impact on wound healing,[60] and the impact of the significant lowering of this, following exposure to CNF materials, needs to be further evaluated together with the other markers of inflammation, coagulation and complement activation. A possible double impact of several cytokines and growth factors has been proposed,[62] and this needs to be investigated further. Since the CNF materials possess an anionic surface and the PDGF-BB has an isoelectric point (pI) of 9.8.[63] , and absorption would possibly explain these data. However, several of the other chemokines and growth factors are also positively charged at neutral pH,[50,64,65] thus this might not fully explain the variability between the chemokine and growth factors. We have previously demonstrated that CNF aerogels incubated with keratinocytes and fibroblasts neither induce cytokines nor growth factors.[22] The current study

represents a more complex system taken into account the reactive cascades of complement and coagulation in collaboration with the leukocytes.[44] Altogether, our explorations indicate a relatively low ability of the CNF materials to potentiate cytokine responses.

The investigated CD11b expression by the leukocyte in response to the CNF materials material points to the potential of activating the leukocytes despite the low cytokine secretion. CD11b is an activation marker improving the phagocytosis ability and cellular-attachment by the leukocytes. Both endotoxins and complement C5a might induce CD11b.[33] Since the present CNF materials were ultrapure, endotoxins can be excluded as the activator. The increased expression CD11b by the porous CNF materials is explainable by the activated complement TCC (C5b-9), since this also generates C5a upon its formation to C5b-9. However, the equal amounts of TCC by the CNF film and PBS control would suggest similar C5a amounts, promoting equal CD11b expression levels. We therefore cannot exclude that activation by additional factors contribute to the increased CD11b expression by the CNF materials. One interesting difference that was apparent between the monocytes and granulocytes when exposed to *E. coli*, was that the monocytes CD11b were most prominent activated. These differences could be connected to the monocyte CD14, which is the co-receptor for LPS. The elevated response of *E. coli* in the monocytes in comparison to granulocytes expression levels could therefore reflect the impact of LPS. Since C5a is a potent inductor of CD11b and rapidly activator,[33] this effector might be the most important that also might have triggered the full potential of activation. This could further explain the lack of differences between the materials as measured after 60 minutes of exposures.

Previously, the cytokine induction have been shown to be connected to surface deposition of C3b/iC3b and cellular attachment through CD11b.[57] Our confocal images demonstrated a

smooth distribution of complement C3, which might indicate an absorption of the native C3 rather than the building of an active C3 convertase. This could both explain the lack of cytokine response as well as the lack of factor H deposition. Interestingly also, MCP-1/CCL2 has previously been shown to be dependent on complement but not to the surface activation by C3b/iC3b deposition,[57] which could be in consistence with the present patterns of fluid phase activation (detected by TCC). One puzzle that remains is however the lack of MCP-1/CCL2 secretion following exposure to AquaCel®, representing the most prominent TCC inductor. MCP-1/CCL2 activation has also been demonstrated to be triggered by nanoparticles of iron oxide in a complement dependent way,[66] and prominently by antibodies to the complement 3 receptor (CR3, CD11b/CD18).[57] One possible explanation for the increased MCP-1/CCL2 activation could therefore be through releasable CNF components activating the fluid phase complement with subsequent binding to CR3 (CD11b/CD18) on the monocytes.

The porosity of CNF materials affects the liquid absorption and the interaction with wound bacteria.[14,22,67] Herein, we demonstrated that the most porous CNF material, the aerogels, induced a rapid and more prominent coagulation response. The rapid coagulation activation points to an involvement by the intrinsic coagulation pathway through FXII, induced by negatively charged surfaces. This is supported by the introduction of carboxyl groups (882 µmol/g) by the oxidation treatment of cellulose.[7] Basu et al.[32] also demonstrated an increase in the FXIIa formation upon exposure to oxidized CNF materials, further supporting this suggestion. Protein activation might also be caused by their structural fitness into nanostructural grooves.[68] Another consideration is the total porosity increased by the porous aerogels in comparison to the films. The CNF material and AquaCel® consist of cellulose with carboxyl-groups and carboxymethyl-groups, respectively. Additionally, the charge of the two materials is different, i.e. 882 and 1350 (µmol/g). Although the CNF material has lower charge

than AquaCel®, the surface that is exposed to the blood is most probably considerably higher for the CNF materials, as can be observed in the SEM images (Fig. 1). CNF dressings swell in liquids[67] and thus increase the exposure of cellulose nanofibrils, which may lead to an increase of the charge density in contact with the blood. Hence, the difference in surface porosity and chemistry might be an explanation for the different activation patterns seen in the two materials. Overall, our data also fits with Leitão et al.[29] showing that porous native bacterial nanocellulose membranes had a quicker clotting time and more complement activation than dried bacterial nanocellulose with less porosity.[29]

The extrinsic pathway of coagulation is involving monocyte tissue factor, which can be induced by endotoxins (as present in *E. coli*), as well as by C5a following biomaterial activation.[36,50] Although we did not investigate the mechanisms in the present study, the strong complement activation by AquaCel® together with the rather slow activation of coagulation, indicate that coagulation is initiated primarily by the extrinsic tissue factor driven pathway with the aid of complement. The rapid increase in PTF1.2 by the CNF aerogels, suggests that the CNF material triggers coagulation through the factor XII dependent intrinsic pathway of coagulation, while also activating complement. The complement activation might further trigger monocyte TF that further could contribute to the coagulation activation.

Activated coagulation factors (FX, IX, XI, thrombin) are shown to directly cleave the central complement components C3 and C5 into functionally activated complement products.[69] Therefore, we cannot exclude the possibility of the complement activation induced by the CNF materials as a result of a direct cleavage by activated coagulation factors. Recent studies however, have questioned the physiological relevance of these data.[70] Altogether, our data indicate that the CNF materials have the potential to induce coagulation, the porous CNF

materials an additional ability to activate complement, while AquaCel® is a main inducer of complement. These differences further suggest that they might have distinct properties in a wound healing situation, or that they could be used at different stages of the wound healing process.

CONCLUSION

This study has assessed the blood coagulation and initial inflammation potential by a carboxylated CNF that is considered ultrapure, i.e. it contains 45 EU/g cellulose. The ultrapure wood CNF materials showed distinct properties in coagulation and complement activation potentials. The aerogels were more potent activators of both coagulation and complement than the CNF film. These differences might be of importance for selecting the most appropriate material in a specific wound healing repair situation, where initiation of coagulation might be beneficial, whereas the complement reactivity might affect the outcome both in a positive or negative direction depending on the chronic wound. Further, the different response profile in comparison to AquaCel® also points to the possibility of creating materials with distinct properties with the possibilities of broader material selections. Although the biomaterials activated leukocytes by CD11b potentiation, a general low cytokine potential and the lowering of distinct chemokines suggest a dampening effect towards specific cytokines of the wound healing materials at the wound site, that only can be further elucidated in wound healing models. The distinct MCP-1/CCL2 induction by the CNF aerogels needs further elucidation of the impact in a wound healing situation. These data as well as the evaluation strategy utilizing human whole blood could be valuable to understand the mechanisms behind the CNF impact in wound healing models, and contribute to tailor wound dressings with the desirable characteristics.

Supporting Information

Overview of the all cytokines and confocal images of the CNF materials with complement inhibitor factor H (PDF). Statistical analyses. Endotoxin assessment of two carboxylated CNF series.

AUTHOR INFORMATION

Corresponding Author

* Gary Chinga-Carrasco, gary.chinga.carrasco@rise-pfi.no

* Anne M. Rokstad, anne.m.rokstad@ntnu.no

Author Contributions

The manuscript was written through contributions of all authors. All authors have given approval to the final version of the manuscript.

ABBREVIATIONS

AFM, atomic force microscope; AG, aerogel; BNC, bacterial nanocellulose; C3, complement factor 3; C5, complement factor 5; CD11b, cluster of differentiation 11b; CD14, cluster of differentiation 14; CD18, cluster of differentiation 18; CNF, cellulose nanofibrils; CR3, complement receptor 3; FGF, fibroblast growth factor; FITC, fluorescein isothiocyanate; FXII, factor XII; IgG, immunoglobulin G; IL, interleukin; IL-1RA, interleukin 1 receptor antagonist; MCP-1, monocyte chemoattractant protein; PDGF-BB, platelet-derived growth factor; PTF1.2, prothrombin factor 1.2; REK, regional ethics committee; S(T)EM, scanning transmission electron microscopy; TCC, terminal complement complex; TEMPO, 2,2,6,6-tetramethylpiperidinyl-1-oxyl; TF, tissue factor; TNF, tumor necrosis factor; VEGF, vascular endothelial growth factor.

REFERENCES

1. Lin, N.; Dufresne, A., Nanocellulose in Biomedicine: Current Status and Future Prospect. Eur. Polym. J. 2014, 59 (0), 302-325.

2. Kollar, P.; Závalová, V.; Hošek, J.; Havelka, P.; Sopuch, T.; Karpíšek, M.; Třetinová, D.; Suchý Jr, P., Cytotoxicity and Effects on Inflammatory Response of Modified Types of Cellulose in Macrophage-like THP-1 cells. Int. Immunopharmacol. 2011, 11 (8), 997-1001.

3. Czaja, W.; Krystynowicz, A.; Bielecki, S.; Brown Jr, R. M., Microbial Cellulose—the Natural Power to Heal Wounds. Biomaterials 2006, 27 (2), 145-151.

4. Dana, K.; Nadine, H., Large-Scale Production of BNC. In Bact. NanoCellul., CRC Press: 2012; pp 43-72.

5. Alexandrescu, L.; Syverud, K.; Gatti, A.; Chinga-Carrasco, G., Cytotoxicity Tests of Cellulose Nanofibril-Based Structures. Cellulose 2013, 1-11.

6. Hua, K.; Ålander, E.; Lindstrom, T.; Mihranyan, A.; Stromme, M.; Ferraz, N., Surface Chemistry of Nanocellulose Fibers Directs Monocyte/Macrophage Response. Biomacromolecules 2015, 16 (9), 2787–2795.

7. Saito, T.; Nishiyama, Y.; Putaux, J.-L.; Vignon, M.; Isogai, A., Homogeneous Suspensions of Individualized Microfibrils from TEMPO-catalyzed Oxidation of Native Cellulose. Biomacromolecules 2006, 7 (6), 1687-1691.

8. Chinga-Carrasco, G., Cellulose fibres, nanofibrils and microfibrils: The Morphological Sequence of MFC Components from a Plant Physiology and Fibre Technology Point of View. Nanoscale Res. Lett. 2011, 6 (1), 1-7.

9. Powell, L. C.; Khan, S.; Chinga-Carrasco, G.; Wright, C. J.; Hill, K. E.; Thomas, D. W., An Investigation of Pseudomonas Aeruginosa Biofilm Growth on Novel Nanocellulose Fibre Dressings. Carbohydr. Polym. 2016, 137, 191-197.

10. Rees, A.; Powell, L. C.; Chinga-Carrasco, G.; Gethin, D. T.; Syverud, K.; Hill, K. E.; Thomas, D. W., 3D Bioprinting of Carboxymethylated-Periodate Oxidized Nanocellulose Constructs for Wound Dressing Applications. BioMed Res. Int. 2015, vol. 2015, 7 pages.

11. Syverud, K.; Kirsebom, H.; Hajizadeh, S.; Chinga-Carrasco, G., Cross-Linking Cellulose Nanofibrils for Potential Elastic Cryo-Structured Gels. Nanoscale Res. Lett. 2011, 6 (1), 1-6.

12. Rashad, A.; Mustafa, K.; Heggset, E. B.; Syverud, K., Cytocompatibility of Wood-Derived Cellulose Nanofibril Hydrogels with Different Surface Chemistry. Biomacromolecules 2017, 18 (4), 1238-1248.

13. Liu, J.; Chinga-Carrasco, G.; Cheng, F.; Xu, W.; Willför, S.; Syverud, K.; Xu, C., Hemicellulose-Reinforced Nanocellulose Hydrogels for Wound Healing Application. Cellulose 2016, 23 (5), 3129-3143.

14. Jack, A. A.; Nordli, H. R.; Powell, L. C.; Powell, K. A.; Kishnani, H.; Johnsen, P. O.; Pukstad, B.; Thomas, D. W.; Chinga-Carrasco, G.; Hill, K. E., The Interaction of Wood Nanocellulose Dressings and the Wound Pathogen P. Aeruginosa. Carbohydr. Polym. 2017, 157, 1955-1962.

15.   Basu, A.; Lindh, J.; Ålander, E.; Strømme, M.; Ferraz, N., On the Use of Ion-Crosslinked Nanocellulose Hydrogels for Wound Healing Solutions: Physicochemical Properties and Application-Oriented Biocompatibility Studies. Carbohydr. Polym. 2017, 174, 299-308.

16.   Basu, A.; Heitz, K.; Strømme, M.; Welch, K.; Ferraz, N., Ion-Crosslinked Wood-Derived Nanocellulose Hydrogels with Tunable Antibacterial Properties: Candidate Materials for Advanced Wound Care Applications. Carbohydr. Polym. 2018, 181, 345-350.

17.   Hua, K.; Carlsson, D. O.; Ålander, E.; Lindström, T.; Strømme, M.; Mihranyan, A.; Ferraz, N., Translational Study Between Structure and Biological Response of Nanocellulose from Wood and Green Algae. RSC Adv. 2014, 4 (6), 2892-2903.

18.   Vartiainen, J.; Pöhler, T.; Sirola, K.; Pylkkänen, L.; Alenius, H.; Hokkinen, J.; Tapper, U.; Lahtinen, P.; Kapanen, A.; Putkisto, K., Health and Environmental Safety Aspects of Friction Grinding and Spray Drying of Microfibrillated Cellulose. Cellulose 2011, 18 (3), 775-786.

19.   Lou, Y.-R.; Kanninen, L.; Kuisma, T.; Niklander, J.; Noon, L. A.; Burks, D.; Urtti, A.; Yliperttula, M., The Use of Nanofibrillar Cellulose Hydrogel as a Flexible Three-Dimensional Model to Culture Human Pluripotent Stem Cells. Stem Cells Dev. 2014, 23 (4), 380-392.

20.   Bhattacharya, M.; Malinen, M. M.; Lauren, P.; Lou, Y.-R.; Kuisma, S. W.; Kanninen, L.; Lille, M.; Corlu, A.; GuGuen-Guillouzo, C.; Ikkala, O.; Laukkanen, A.; Urtti, A.; Yliperttula, M., Nanofibrillar Cellulose Hydrogel

Promotes Three-Dimensional Liver Cell Culture. J. Controlled Release 2012, 164 (3), 291-298.

21.   Malinen, M. M.; Kanninen, L. K.; Corlu, A.; Isoniemi, H. M.; Lou, Y.-R.; Yliperttula, M. L.; Urtti, A. O., Differentiation of Liver Progenitor Cell Line to Functional Organotypic Cultures in 3D Nanofibrillar Cellulose and Hyaluronan-Gelatin Hydrogels. Biomaterials 2014, 35 (19), 5110-5121.

22.   Nordli, H. R.; Chinga-Carrasco, G.; Rokstad, A. M.; Pukstad, B., Producing Ultrapure Wood Cellulose Nanofibrils and Evaluating the Cytotoxicity Using Human Skin Cells. Carbohydr. Polym. 2016, 150, 65-73.

23.   Reinke, J.; Sorg, H., Wound Repair and Regeneration. Eur. Surg. Res. 2011, 49 (1), 35-43.

24.   Franz, S.; Rammelt, S.; Scharnweber, D.; Simon, J. C., Immune Responses to Implants – A Review of the Implications for the Design of Immunomodulatory Biomaterials. Biomaterials 2011, 32 (28), 6692-6709.

25.   Nilsson, B.; Ekdahl, K. N.; Mollnes, T. E.; Lambris, J. D., The Role of Complement in Biomaterial-Induced Inflammation. Mol. Immunol. 2007, 44 (1–3), 82-94.

26.   Sinno, H.; Prakash, S., Complements and the Wound Healing Cascade: an Updated Review. Plastic surgery international 2013, 2013, 7 pages.

27.   Cazander, G.; Jukema, G. N.; Nibbering, P. H. J., Complement Activation and Inhibition in Wound Healing. Clin. Dev. Immunol. 2012, 2012, 14 pages.

28.   Andrade, F. K.; Silva, J. P.; Carvalho, M.; Castanheira, E. M. S.; Soares, R.; Gama, M., Studies on the Hemocompatibility of Bacterial Cellulose. Biomed. Mater. Res., Part A 2011, 98A (4), 554-566.

29.   Leitão, A. F.; Gupta, S.; Silva, J. P.; Reviakine, I.; Gama, M., Hemocompatibility Study of a Bacterial Cellulose/Polyvinyl Alcohol Nanocomposite. Colloids Surf., B 2013, 111, 493-502.

30.   Fink, H.; Hong, J.; Drotz, K.; Risberg, B.; Sanchez, J.; Sellborn, A., An in Vitro Study of Blood Compatibility of Vascular Grafts made of Bacterial Cellulose in Comparison with Conventionally-Used Graft Materials. J. Biomed. Mater. Res., Part A 2011, 97A (1), 52-58.

31.   Fink, H.; Faxälv, L.; Molnár, G. F.; Drotz, K.; Risberg, B.; Lindahl, T. L.; Sellborn, A., Real-Time Measurements of Coagulation on Bacterial Cellulose and Conventional Vascular Graft Materials. Acta Biomater. 2010, 6 (3), 1125-1130.

32.   Basu, A.; Hong, J.; Ferraz, N., Hemocompatibility of Ca2+-Crosslinked Nanocellulose Hydrogels: Toward Efficient Management of Hemostasis. Macromol. Biosci. 2017, 17 (11), 1700236.

33.   Mollnes, T. E.; Brekke, O.-L.; Fung, M.; Fure, H.; Christiansen, D.; Bergseth, G.; Videm, V.; Lappegård, K. T.; Köhl, J.; Lambris, J. D., Essential Role of the C5a Receptor in E coli–Induced Oxidative Burst and Phagocytosis Revealed by a Novel Lepirudin-Based Human Whole Blood Model of Inflammation. Blood 2002, 100 (5), 1869-1877.

34.   Rokstad, A. M.; Brekke, O.-L.; Steinkjer, B.; Ryan, L.; Kolláriková, G.; Strand, B. L.; Skjåk-Bræk, G.; Lacík, I.; Espevik, T.; Mollnes, T. E., Alginate

Microbeads are Complement Compatible, in Contrast to Polycation Containing Microcapsules, as Revealed in a Human Whole Blood Model. Acta Biomater. 2011, 7 (6), 2566-2578.

35.   Rokstad, A. M.; Brekke, O.-L.; Steinkjer, B.; Ryan, L.; Kolláriková, G.; Strand, B. L.; Skjåk-Bræk, G.; Lambris, J. D.; Lacík, I.; Mollnes, T. E.; Espevik, T., The Induction of Cytokines by Polycation Containing Microspheres by a Complement Dependent Mechanism. Biomaterials 2013, 34 (3), 621-630.

36.   Gravastrand, C.; Hamad, S.; Fure, H.; Steinkjer, B.; Ryan, L.; Oberholzer, J.; Lambris, J. D.; Lacík, I.; Mollnes, T. E.; Espevik, T.; Brekke, O.-L.; Rokstad, A. M., Alginate Microbeads are Coagulation Compatible, While Alginate Microcapsules Activate Coagulation Secondary to Complement or Directly Through FXII. Acta Biomater. 2017, 58 (Supplement C), 158-167.

37.   Mollnes, T. E.; Redl, H.; Hogasen, K.; Bengtsson, A.; Garred, P.; Speilberg, L.; Lea, T.; Oppermann, M.; Gotze, O.; Schlag, G., Complement Activation in Septic Baboons Detected by Neoepitope-Specific Assays for C3b/iC3b/C3c, C5a and the Terminal C5b-9 Complement Complex (TCC). Clin. Exp. Immunol. 1993, 91 (2), 295-300.

38.   Chinga-Carrasco, G.; Kuznetsova, N.; Garaeva, M.; Leirset, I.; Galiullina, G.; Kostochko, A.; Syverud, K., Bleached and Unbleached MFC Nanobarriers: Properties and Hydrophobisation with Hexamethyldisilazane. J. Nanopart. Res.2012, 14 (12), 1-10.

39.   Saito, T.; Isogai, A., TEMPO-Mediated Oxidation of Native Cellulose. The Effect of Oxidation Conditions on Chemical and Crystal Structures of the Water-Insoluble Fractions. Biomacromolecules 2004, 5 (5), 1983-1989.

40.   Queen, D., Technology update: Understanding hydrocolloids. Wounds International 2010, 1 (1).

41.   Lappegård, K. T.; Christiansen, D.; Pharo, A.; Thorgersen, E. B.; Hellerud, B. C.; Lindstad, J.; Nielsen, E. W.; Bergseth, G.; Fadnes, D.; Abrahamsen, T. G.; Høiby, E. A.; Schejbel, L.; Garred, P.; Lambris, J. D.; Harboe, M.; Mollnes, T. E., Human Genetic Deficiencies Reveal the Roles of Complement in the Inflammatory Network: Lessons from Nature. Proc. Natl. Acad. Sci. U. S. A. 2009, 106 (37), 15861-15866.

42.   Samstad, E. O.; Niyonzima, N.; Nymo, S.; Aune, M. H.; Ryan, L.; Bakke, S. S.; Lappegård, K. T.; Brekke, O.-L.; Lambris, J. D.; Damås, J. K.; Latz, E.; Mollnes, T. E.; Espevik, T., Cholesterol Crystals Induce Complement-Dependent Inflammasome Activation and Cytokine Release. J. Immunol. 2014, 192 (6), 2837-2845.

43.   Landsem, A.; Fure, H.; Christiansen, D.; Nielsen, E. W.; Østerud, B.; Mollnes, T. E.; Brekke, O. L., The Key Roles of Complement and Tissue Factor in Escherichia Coli-Induced Coagulation in Human Whole Blood. Clin. Exp. Immunol. 2015, 182 (1), 81-89.

44.   Rokstad, A. M.; Strand, B.; Espevik, T.; Mollnes, T. E., Biocompatibility and Biotolerability Assessment of Microspheres Using a Whole Blood Model. Micro Nanosyst. 2013, 5, 177-185.

45.	Ricklin, D.; Hajishengallis, G.; Yang, K.; Lambris, J. D., Complement: a Key System for Immune Surveillance and Homeostasis. Nat. Immunol. 2010, 11 (9) 785-797.

46.	Hajishengallis, G.; Lambris, J. D., More than complementing Tolls: Complement-Toll-Like Receptor Synergy and Crosstalk in Innate Immunity and Inflammation. Immunol. Rev. 2016, 274 (1), 233-244.

47.	Mollnes, T. E.; Lea, T.; Harboe, M., Detection and Quantification of the Terminal C5b-9 Complex of Human Complement by a Sensitive Enzyme-Linked Immunosorbent Assay. Scand. J. Immunol. 1984, 20 (2), 157-166.

48.	Mollnes, T.; Redl, H.; Høgåsen, K.; Bengtsson, A.; Garrhd, P.; Speilberg, L.; Lea, T.; Oppermann, M.; Götze, O.; Schlag, G., Complement Activation in Septic Baboons Detected by Neoepitope-Specific Assays for C3b/iC3b/C3c, C5a and the Terminal C5b-9 Complement Complex (TCC). Clin. Exp. Immunol. 1993, 91 (2), 295-300.

49.	Chinga-Carrasco, G.; Yu, Y.; Diserud, O., Quantitative Electron Microscopy of Cellulose Nanofibril Structures from Eucalyptus and Pinus radiata Kraft Pulp Fibers. Microsc. Microanal.2011, 17 (04), 563-571.

50.	Brekke, O.; Waage, C.; Christiansen, D.; Fure, H.; Qu, H.; Lambris, J. D.; Østerud, B.; Nielsen, E.; Mollnes, T., The Effects of Selective Complement and CD14 Inhibition on the E. coli-Induced Tissue Factor mRNA Upregulation, Monocyte Tissue Factor Expression, and Tissue Factor Functional Activity in Human Whole Blood. In Complement Therapeutics, Lambris, J.; Holers, V.; Ricklin, D., Eds. Springer: 2013; Vol. 735, pp 123-136.

51. Gros, P.; Milder, F. J.; Janssen, B. J., Complement Driven by Conformational Changes. Nat. Rev. Immunol. 2008, 8 (1), 48-58.

52. Arlov, Ø.; Skjåk-Bræk, G.; Rokstad, A. M., Sulfated Alginate Microspheres Associate with Factor H and Dampen the Inflammatory Cytokine Response. Acta Biomater. 2016, 42 (Supplement C), 180-188.

53. Gustavsen, A.; Nymo, S.; Landsem, A.; Christiansen, D.; Ryan, L.; Husebye, H.; Lau, C.; Pischke, S. E.; Lambris, J. D.; Espevik, T.; Mollnes, T. E., Combined Inhibition of Complement and CD14 Attenuates Bacteria-Induced Inflammation in Human Whole Blood More Efficiently Than Antagonizing the Toll-like Receptor 4–MD2 Complex. J. Infect. Dis. 2016, 214 (1), 140-150.

54. Barratt-Due, A.; Pischke, S. E.; Brekke, O.-L.; Thorgersen, E. B.; Nielsen, E. W.; Espevik, T.; Huber-Lang, M.; Mollnes, T. E., Bride and Groom in Systemic Inflammation – The Bells Ring for Complement and Toll in Cooperation. Immunobiology 2012, 217 (11), 1047-1056.

55. Martoïa, F.; Cochereau, T.; Dumont, P. J. J.; Orgéas, L.; Terrien, M.; Belgacem, M. N., Cellulose Nanofibril Foams: Links Between Ice-Templating Conditions, Microstructures and Mechanical Properties. Mater. Des. 2016, 104, 376-391.

56. Lappegård, K. T.; Bergseth, G.; Riesenfeld, J.; Pharo, A.; Magotti, P.; Lambris, J. D.; Mollnes, T. E., The Artificial Surface-Induced Whole Blood Inflammatory Reaction Revealed by Increases in a Series of Chemokines and Growth Factors is Largely Complement Dependent. J. Biomed. Mater. Res., Part A 2008, 87A (1), 129-135.

57. Ørning, P.; Hoem, K. S.; Coron, A. E.; Skjåk-Bræk, G.; Mollnes, T. E.; Brekke, O.-L.; Espevik, T.; Rokstad, A. M., Alginate Microsphere Compositions Dictate Different Mechanisms of Complement Activation with Consequences for Cytokine Release and Leukocyte Activation. J. Controlled Release 2016, 229 (Supplement C), 58-69.

58. Gorbet, M. B.; Sefton, M. V., Endotoxin: The Uninvited Guest. Biomaterials 2005, 26 (34), 6811-6817.

59. L., B. C.; J., A. C., Normal Cutaneous Wound Healing: Clinical Correlation with Cellular and Molecular Events. Dermatol. Surg. 2005, 31 (6), 674-686.

60. Smiell, J. M.; Wieman, T. J.; Steed, D. L.; Perry, B. H.; Sampson, A. R.; Schwab, B. H., Efficacy and Safety of Becaplermin (Recombinant Human Platelet-Derived Growth Factor-BB) in Patients with Nonhealing, Lower Extremity Diabetic Ulcers: a Combined Analysis of Four Randomized Studies. Wound Repair and Regeneration 1999, 7 (5), 335-346.

61. Hogan, S. P.; Rosenberg, H. F.; Moqbel, R.; Phipps, S.; Foster, P. S.; Lacy, P.; Kay, A. B.; Rothenberg, M. E., Eosinophils: Biological Properties and Role in Health and Disease. Clin. Exp. Allergy 2008, 38 (5), 709-750.

62. Ligi, D.; Mosti, G.; Croce, L.; Raffetto, J. D.; Mannello, F., Chronic Venous Disease – Part I: Inflammatory Biomarkers in Wound Healing. Biochim. Biophys. Acta, Mol. Basis Dis. 2016, 1862 (10), 1964-1974.

63. Antoniades, H. N.; Scher, C. D.; Stiles, C. D., Purification of Human Platelet-Derived Growth Factor. Proc. Natl. Acad. Sci. U. S. A. 1979, 76 (4), 1809-1813.

64. Helmy, A.; Carpenter, K. L. H.; Skepper, J. N.; Kirkpatrick, P. J.; Pickard, J. D.; Hutchinson, P. J., Microdialysis of Cytokines: Methodological Considerations, Scanning Electron Microscopy, and Determination of Relative Recovery. Journal of Neurotrauma 2009, 26 (4), 549-561.

65. Yang, D.; Chen, Q.; Hoover, D. M.; Staley, P.; Tucker, K. D.; Lubkowski, J.; Oppenheim, J. J., Many Chemokines Including CCL20/MIP-3α Display Antimicrobial Activity. J. Leukocyte Biol. 2003, 74 (3), 448-455.

66. Wolf-Grosse, S.; Rokstad, A. M.; Ali, S.; Lambris, J. D.; Mollnes, T. E.; Nilsen, A. M.; Stenvik, J., Iron Oxide Nanoparticles Induce Cytokine Secretion in a Complement-Dependent Manner in a Human Whole Blood Model. Int. J. Nanomed. 2017, 12, 3927-3940.

67. Sun, F.; Nordli, H. R.; Pukstad, B.; Kristofer Gamstedt, E.; Chinga-Carrasco, G., Mechanical Characteristics of Nanocellulose-PEG Bionanocomposite Wound Dressings in Wet Conditions. J. Mech. Behav. Biomed. Mater. 2017, 69, 377-384.

68. Ferraz, N.; Nilsson, B.; Hong, J.; Ott, M. K., Nanoporesize Affects Complement Activation. J. Biomed. Mater. Res., Part A 2008, 87A (3), 575-581.

69. Amara, U.; Flierl, M. A.; Rittirsch, D.; Klos, A.; Chen, H.; Acker, B.; Brückner, U. B.; Nilsson, B.; Gebhard, F.; Lambris, J. D.; Huber-Lang, M., Molecular Intercommunication between the Complement and Coagulation Systems. J. Immunol. 2010, 185 (9), 5628-5636.

70. Keshari, R. S.; Silasi, R.; Lupu, C.; Taylor, F. B.; Lupu, F., In Vivo–Generated Thrombin and Plasmin do not Activate the Complement System in Baboons. Blood 2017, 130 (24), 2678-2681.

TABLE OF CONTENTS GRAPHIC

42